On the Importance of Intermediate Internal Charge Repulsion for the Synthesis of Multifunctional Pores[1])

by **Bodo Baumeister**[a])[2]), **Abhigyan Som**[a]), **Gopal Das**[a]), **Naomi Sakai**[a]), **Francis Vilbois**[b]), **David Gerard**[a]), **Shatrughan P. Shahi**[a]), and **Stefan Matile***[a])

[a]) Department of Organic Chemistry, University of Geneva, CH-1211 Geneva 4
[b]) *Serono Pharmaceutical Research Institute*, CH-1228 Plan-les-Ouates, Geneva

Dedicated to Prof. *Wolf-Dietrich Woggon* on the occasion of his 60th birthday

Intermediate internal charge repulsion (*ICR*) is required to create synthetic pores with large, stable, transmembrane, and variably functionalized space. This conclusion is drawn from maximal transport and, in one case, catalytic activity of *p*-octiphenyl β-barrel pores with internal lysine, aspartate, and histidine residues around pH 7, 6, and 4.5, respectively. pK_a Simulations corroborate the experimental correlation of intermediate *ICR* with activity and suggest that insufficient *ICR* causes pore 'implosion' and excess *ICR* pore 'explosion'. Esterolysis experiments support the view that the formation of stable space within multifunctional *p*-octiphenyl β-barrels requires more *ICR* in bilayer membranes than in H_2O. Multivalency effects are thought to account for *p*-octiphenyl β-barrel expansion with increasing number of β-sheets, and proximity effects for unchanged pH profiles with increasing β-sheet length. Q-TOF-nano-ESI-MS barrel-denaturation experiments indicate that contributions from internal counterion effects are not negligible. The overall characteristics of *p*-octiphenyl β-barrel pores with internal lysine, aspartate, and histidine residues, unlike *de novo* 'α-barrels' and similarly to certain biological channels, underscore the usefulness of rigid-rod molecules to preorganize complex multifunctional supramolecular architecture.

Introduction. – The rational design of functional ion channels and pores from first principles [1–5] has seen much progress since the initial studies by *Tabushi*, *Besch*, and co-workers [4]. Despite these substantial efforts, the design of specific host-guest interactions within synthetic ion channels and pores remains a recognized [5] but largely unexplored challenge in bioorganic chemistry. Facile access to transmembrane, large, and stable synthetic ion channels with variable internal active sites is, however, a prerequisite for future (bioorganic) chemistry within the confined space of synthetic multifunctional pores. This is an attractive objective because the spatial compartmentalization by liquid crystalline bilayer templates introduces, *in principle*, vectorial control over initiation and topological control over propagation and termination of chemical processes within synthetic pores and, as demonstrated with biological pores [6], detectability at the single-molecule level [7]. In previous work [8–17], we have shown that rigid-rod [18] β-barrels [19] offer the first general approach to the synthesis of self-assembled ion channels and pores with variable internal active sites beyond *de novo* α-helix bundles [20–23]. Here, we use pH profiles and pK_a simulations for *p*-octiphenyl β-barrels **1**–**6** with internal lysine (K), histidine (H), and aspartate (D)

---

1) Part of this work has been published previously in the Ph.D. thesis [1].
2) Current address: *Calbiochem-Novabiochem AG*, Weidenmattweg 4, CH-4448 Läufelfingen.

residues to evaluate the importance of internal charge repulsion (*ICR*) to create transmembrane, stable, large, and functionalized space (*Figs. 1* and *2*). The results, summarized as the *ICR* model, suggest that lack of *ICR* causes 'implosion', low *ICR* contraction, high *ICR* expansion, and excess *ICR* 'explosion' of barrel-stave supramolecules (*Fig. 1*).

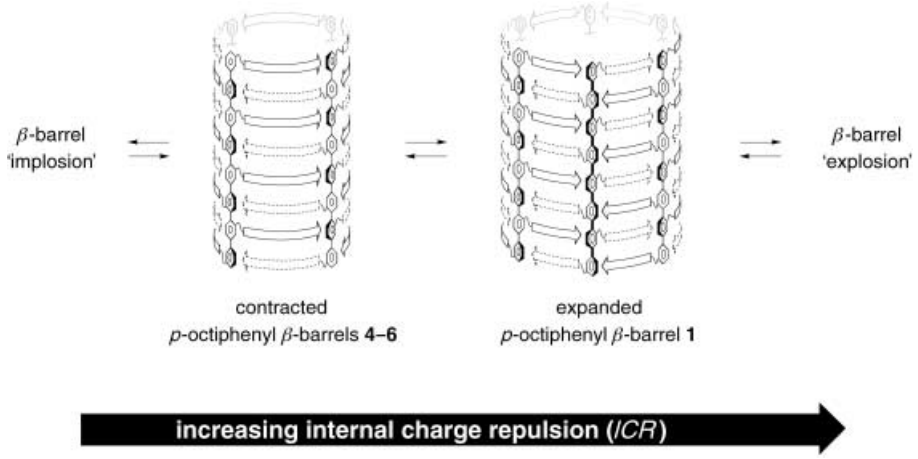

Fig. 1. *The internal charge repulsion* (*ICR*) *model*. Lack of *ICR* is thought to account for 'implosion', low *ICR* for contraction, high *ICR* for expansion, and excess *ICR* for 'explosion' of barrel-stave supramolecules. Details on β-sheet (arrows) and *p*-octiphenyl structure in β-barrels **1**–**6** are given in *Figs. 2* and *3*.

Results and Discussion. – The influence of spacial proximity of multiply charged acids and bases on the individual $pK_a(i)$ of acid/base *i* can be simulated by *Eqn. 1*, which assumes additivity of contributions from intrinsic pK_a (pK_a'), probability of proton transfer ($\log(\Omega_{i-1}/\Omega_i)$), and electrostatic repulsion between charged bases like carboxylate anions of aspartate ($\gamma = +1$) and charged acids like ammonium cations in lysine ($\gamma = -1$) [24]. The probability term $\log(\Omega_{i-1}/\Omega_i)$ describes the possibilities to add or remove $1 \leq i \leq n$ protons for *n* sites (see *Eqn. 2*). The average electrostatic repulsion G_r between two charges depends on several parameters including average distance ($G_r \propto r^{-2}$) but also on the relative permittivity of the medium and counterion binding constants.

$$pK_a(i) = pK_a' + \gamma\log(\Omega_{i-1}/\Omega_i) + \gamma(i-1)G_r/2.303RT \quad (1)$$

$$\Omega_i = n!\,/\,(n-i)!\,i! \quad (2)$$

Eqn. 1 has been applied previously to rationalize pH-dependent changes in ion selectivity of alamethicin ion channels with one additional lysine per α-helix in an 'α-barrel' of eight α-helices [24]. As *Woolley* and co-workers, we decided to use the known $pK_a(i)$ of azacrowns **7** and **8** (◆ and ■, resp., in *Fig. 3*) for an approximation of G_r [25]. Assuming an intrinsic $pK_a' = 10.5$, simulation of experimental $pK_a(i)$ gave best results with $G_r = 1.0$ kcal/mol for contracted azacrown **7** (dotted line) and $G_r = 0.7$ kcal/mol for

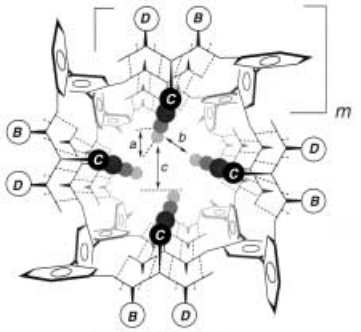

1–5 (axial view)

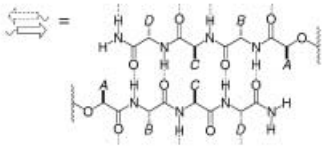

	A - B - C - D	m	n
1	G - L - K - L	3	48
2[a)]	G - L - K - L	1	24
3[b)]	G - L - K - L	1	24
5	G - L - H - L	1	32

a) $1^4,8^4$-Dimethoxy-substituted (see *Fig. 3*).
b) 1^4-Methoxy-8^4-(methylsulfonyl)-substituted (see *Fig. 3*).

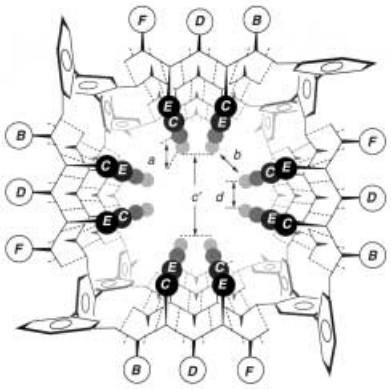

4–6 (axial view)

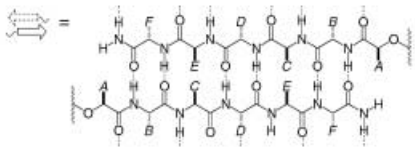

	A - B - C - D - E - F	n
4	G - L - D - L - D - L	64
6	G - L - H - L - H - L	64

Fig. 2. *Axial view and peptide sequences of the* p-*octiphenyl* β-*barrels* **1**–**6** *from* Fig. 1 (8-stranded) *and* Fig. 3 (6-stranded). One-letter abbreviations are used for amino acids (L = Leu, K = Lys, H = His, D = Asp; G = $-OCH_2CO-$). n = number of acid/bases per supramolecule. In molecular models [9], internal distances are $a \approx 5$ Å, $b \approx 4$ Å (**1**: *ca.* 12 Å), $c \approx 7$ Å (**1**: *ca.* 23 Å), $c' \approx 14$ Å, and $d \approx 7$ Å.

expanded azacrown **8** (solid line). This difference in G_r originates presumably from the increased average distance r between two positive charges.

The comparison with the known $pK_a(i)$ of azacrowns **7** and **8** provided a semiquantitative entry for the development of an *ICR* model for synthetic pores formed by rigid-rod β-barrels and perhaps other barrel-stave supramolecules. For convenience and clarity only, internal charge excess ICE_{pH} of an active pore was defined as being equal to the number of internal charged acids/bases i at given pH, and internal charge repulsion ICR_{pH} by *Eqn. 3*.

$$ICR_{pH} = ICE_{pH}\, G_r \tag{3}$$

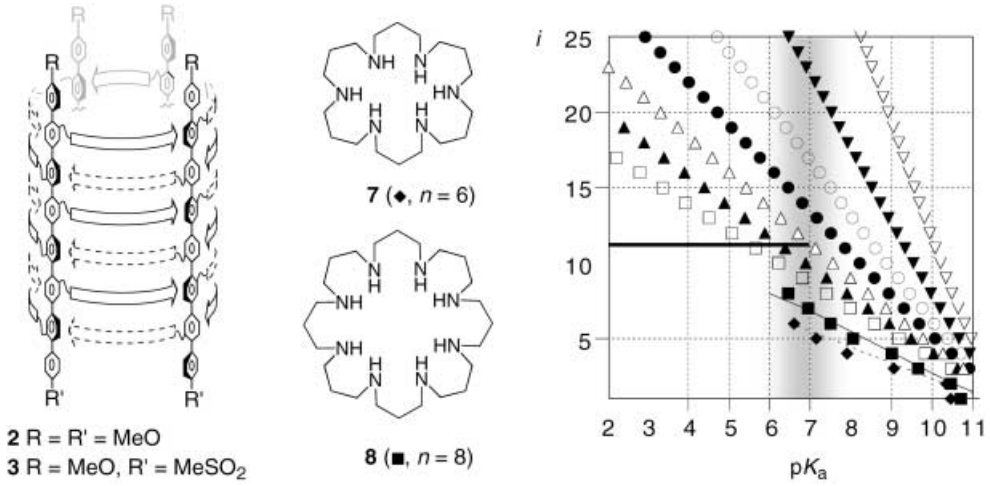

Fig. 3. *The* ICR *between internal lysine residues. Experimental* (◆ and ■, see [25]) *and simulated* pK_a *values for azacrowns* **7** (----: $G_r = 1.0$ kcal/mol) *and* **8** (—: $G_r = 0.7$ kcal/mol) *and simulated* pK_a *values for* p-*octiphenyl* β-*barrels* **1**–**3** (*cf. Fig. 2*) *with* pK_a *range* (gray) *and* $ICE_{pH} \approx 11$ (—) *relevant for* **2** and **3** ($n = 32$, $pK'_a = 10.5$, $G_r =$ 0.7 (□), 0.6 (▲), 0.5 (△), 0.4 (●), 0.3 (○), 0.2 (▼), and 0.1 kcal/mol (▽)). i = number of protonation sites.

Evidently, the *ICR* model is, at best, an approximation and, in part, a speculative working hypothesis. Contributions from, *e.g.*, barrel-specific intrinsic pK_as as well as barrel-specific counterion effects on absolute $pK_a(i)$s were not considered. Since the increase from $n = 8$ for azacrown **8** to $n = 32$ had relatively little influence on the first eight pK_as simulated for $G_r = 0.7$ kcal/mol (*Fig. 3*, □ *vs.* ■), we further decided to use $n = 32$ as representative for high multivalency in all barrels to simplify comparisons. With these reservations in mind, the *ICR* model proposed in *Fig. 1* was evaluated by comparing experimental characteristics, simulated $pK_a(i)$s, and calculated ICE_{pH} and ICR_{pH} of synthetic multifunctional pores **1**–**6**.

Barrels with Internal Lysine Residues. Tetrameric rigid-rod β-barrels **2** and **3** form transmembrane, stable, and large anion channels at pH ≈ 7 [8]. The internal-lysine amino groups are expected to be regularly placed at the inner barrel surface with *ca.* 5 Å vertical separation (*a* in *Fig. 2*), *ca.* 4 Å horizontal separation at *p*-oligophenyl turns (*b*), and *ca.* 7 Å horizontal separation across the channel (*c*) [9]. The *local* average distance *r* between two ammonium cations in tetramers **2** and **3** are thus the same as or not much longer than in azacrown **8**, *i.e.*, *local* $G_r \approx 0.7$ kcal/mol. The *global* average distance *r* between two ammonium cations in the entire supramolecules **2** and **3** considered in *Eqn. 1*, however, must be clearly longer than in **8** because the most distant cations are separated by up to 26 Å. Reduction of *global* G_r from $G_r = 0.7$ kcal/mol (□) to $G_r = 0.1$ kcal/mol (▽) caused a strong increase of all $pK_a(i)$s (*Fig. 3*). At pH *ca.* 7, this approximative simulation indicated half and full protonation of **2** and **3** for $G_r \approx$ 0.5 kcal/mol (△) and $G_r \approx 0.2$ kcal/mol (▼), respectively. Since internal overcharge causes barrel 'explosion' (see below), an approximative G_r of 0.5 kcal/mol (*Fig. 3*, △) giving $ICE_{7.0} \approx 11$ and $ICR_{7.0} \approx 6$ kcal/mol may characterize transmembrane, stable, and large anion channels formed by tetramers **2** and **3** reasonably well (*Fig. 2*).

Hexameric rigid-rod β-barrel **1** with internal lysine moieties forms transmembrane and stable ion channels [10] with an internal space large enough to bind oligonucleotide duplexes in B-DNA conformation [11]. Transition from 6-stranded β-sheets in barrels **2** and **3** to 8-stranded β-sheets in barrel **1** thus results, at pH $\approx$ 7, in barrel expansion from tetramers to hexamers.

This barrel expansion may be better understood considering *Eqn. 1*. Namely, formal addition of two far-apart β-strand 'hoops' in tetramers **2** and **3** will reduce the *global* $G_r \approx 0.5$ kcal/mol ($\triangle$ in *Fig. 3*). Reduction of G_r will, in turn, increase the $ICE_{7.0} \approx 11$ of **2** and **3** ($\triangle$) to $ICE_{7.0} \approx 14$ with $G_r \approx 0.4$ kcal/mol ($\bullet$), $ICE_{7.0} \approx 17$ with $G_r \approx 0.3$ kcal/mol ($\circ$), $ICE_{7.0} \approx 24$ with $G_r \approx 0.2$ kcal/mol ($\blacktriangledown$), and so on. Increase of *ICE* without compensating decrease of *local* G_r will, however, build up internal overcharge that is ultimately released by expansion into hexamer **1** with reduced *local* G_r. In hexamer **1**, half protonation reached around $G_r \approx 0.2$ kcal/mol ($\blacktriangledown$) indicated $ICE_{7.0} \approx 24$ and $ICR_{7.0} \approx 5$ kcal/mol, *i.e.*, increased $ICE_{7.0}$ but about maintained *ICR* compared to tetramers **2** and **3**. Barrel expansion, overall, can thus be understood as a multivalency rather than proximity effect.

The pH profile of lysine-rich hexamer **1** in small unilamellar vesicles composed of egg-yolk phosphatidylcholine (EYPC SUVs) was determined by means of the ANTS/DPX-leakage assay as described previously for aspartate-rich tetramer **4** [12]. In brief, EYPC SUVs were loaded with anionic fluorophore ANTS (= 8-aminonaphthalene-1,3,6-trisulfonic acid disodium salt) and cationic quencher DPX (= 1,1′-[1,4-phenylenebis(methylene)]bis[pyridinium]bromide) (*Fig. 4*). Efflux of either ANTS or DPX through pores formed by rigid-rod β-barrel **1** was followed by an increase in ANTS emission intensity. The ANTS/DPX assay was ideal for determination of pH profiles because ANTS emission is pH-independent and ANTS/DPX efflux does not depend strongly on changes in ion selectivity with pH. Decreasing activity of hexamer **1** with decreasing pH (*Fig. 4*) was consistent with barrel 'explosion' at excess *ICR* (*cf. Fig. 1*). Although not studied at the structural level, barrel 'explosion' most likely produces highly charged monomers that are too hydrophilic to partition to the membrane.

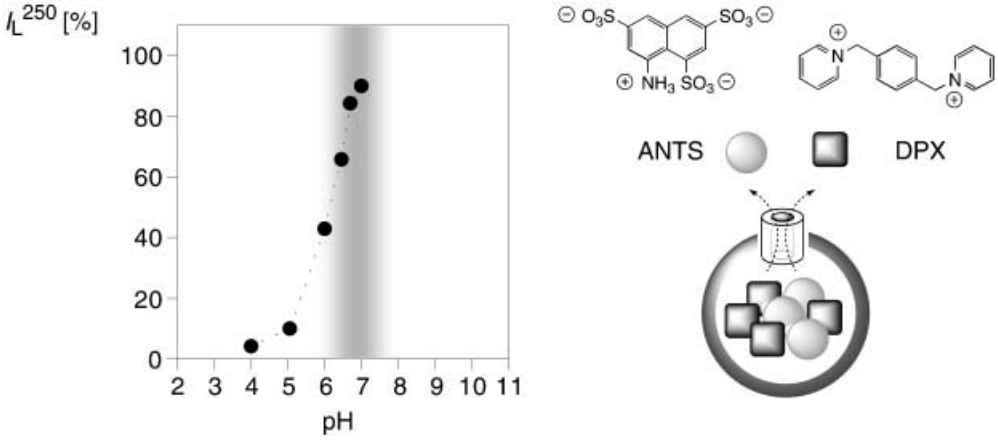

Fig. 4. *The* ICR *between internal lysine residues. Experimental pH profile for* p-*octiphenyl* β*-barrel* **1** (110 nM) *in EYPC-SUVs and schematic description of the ANTS/DPX assay.* I_L^{250} according to *Eqn. 4* (*Exper. Part*).

Barrels with Internal Aspartate Residues. Tetrameric rigid-rod β-barrels **4** form doubly pH-gated pores at $5 < pH < 7$ with an internal space large enough to bind Mg^{2+}-complexed ANTS (*cf. Fig. 2*) [12]. Compared to tetramers **2** and **3** with 6-stranded β-sheets formed by tripeptides, rigid-rod β-barrels **4** contain 8-stranded β-sheets formed by pentapeptides. This β-sheet elongation by *ca.* 7 Å (*d* in *Fig. 2*) should place the G_r of 'pentapeptide' tetramer **4** between those approximated for 'tripeptide' tetramers **2** and **3** ($G_r \approx 0.5$ kcal/mol, △) and 'tripeptide' hexamer **1** ($G_r \approx 0.2$ kcal/mol, ▼). These two extreme situations were simulated with *Eqn. 1*, assuming an intrinsic pK_a' of 4.5 (*Fig. 5*). Comparison with the experimental pH profile (*Fig. 5*, ●) indicated that an intermediate $7 < ICE_{6.0} < 12$ accounts for active pores **4**, whereas a poor $ICE_{5.0} < 7$ and excessive $ICE_{7.0} > 12$ gives inactive pores due to barrel implosion and explosion, respectively (*cf. Fig. 1*).

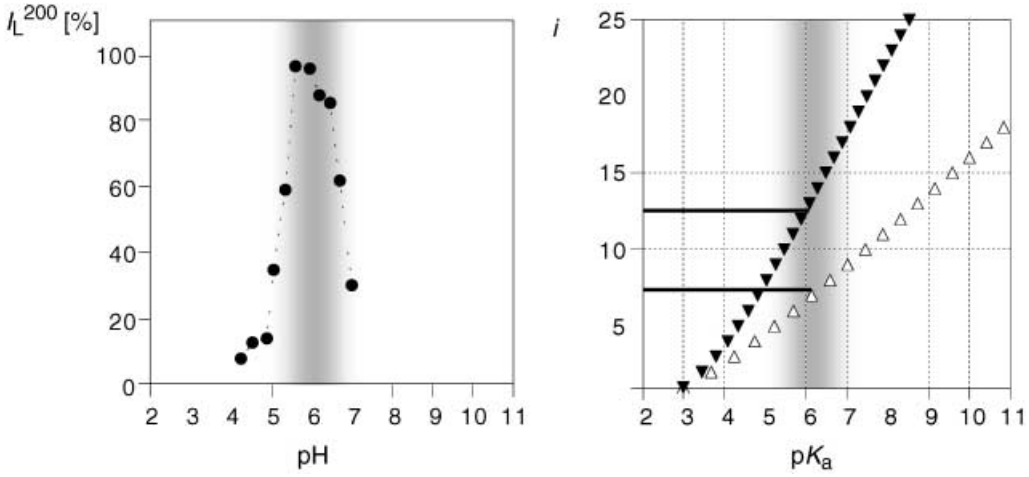

Fig. 5. *The* ICR *between internal aspartate residues. Experimental pH profile for* p-*octiphenyl* β*-barrel* **4** (●, [12]) *in EYPC SUVs and simulated* pK_a *values for* $G_r = 0.5$ (△) *and 0.2 kcal/mol* (▼) *with relevant pH/*pK_a *range* (gray) *and* $7 < ICE_{pH} < 12$ (—; $n = 32$, $pK_a' = 4.5$). I_L^{200} according to *Eqn. 4* (*Exper. Part*), i = number of protonation sites.

Barrels with Internal Histidine Residues. According to the *Hille* model [26], the conductance of stable single channels **5** [13], similar to that of stable tetramers **2** and **3** [8] but clearly smaller than that of stable hexamers **1** [10], demonstrates that histidine-rich rigid-rod β-barrels **5** are stable tetramers at pH 5. The pH profile of pore formation by histidine-rich tetramer **5** in EYPC SUVs was determined by using the ANTS/DPX assay described above (*cf. Fig. 4*). It revealed maximal activity at $pH \leq 5$ (*Fig. 6*, ●).

Selective pore formation of cationic β-barrels **5** around pH 4.5 was simulated under the conditions discussed for anionic β-barrels **4**, *i.e.*, 0.2 (▼) $\leq G_r \leq 0.5$ kcal/mol (△) and an intrinsic $pK_a' = 6.0$ (*Fig. 6*). Comparison of the pH profile and pK_a simulations indicated that intermediate $7 < ICE_{5.0} < 12$ accounts for active pores **5**, whereas poor $ICE_{6.0} < 7$ causes barrel implosion. Remarkably, about the same intermediate *ICR* at different pH, therefore, activates anionic and cationic β-barrels **4** and **5** with, judged from the sharp transitions, high cooperativity. Absence of barrel expansion with

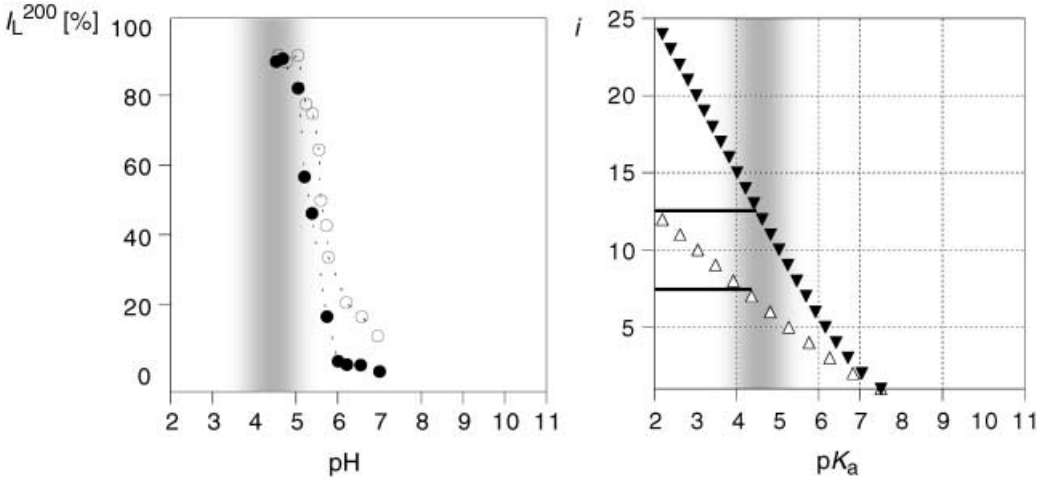

Fig. 6. *The* ICR *between internal histidine residues. Experimental pH profile for* p-*octiphenyl β-barrel* **5** (●) *and* **6** (○) *and simulated* pK_a *values for* $G_r = 0.5$ (△) *and 0.2 kcal/mol* (▼) *with relevant pH/*pK_a *range* (gray) *and* $7 < ICE_{pH} < 12$ (—; $n = 32$, p$K_a = 6.0$). I_L^{200} according to *Eqn. 4* (*Exper. Part*), i = number of protonation sites.

tetramer **5** as for hexamer **1** suggested weaker multivalency effects with internal histidine residues compared to lysine residues (*i.e.*, that the *local* G_r between protonated internal histidine residues is lower than that between internal lysine residues, presumably because of charge delocalization and, perhaps, reduced amino acid side-chain length).

Tetrameric rigid-rod *β*-barrel **6** forms large, *labile* ion channels at pH 5.0 in bilayer membranes [14], has esterase activity in H_2O and bilayer membranes [14], and RNase [15] and fibrillogenic activity [16] in H_2O. The pH profile of *β*-barrel **6** was similar to that of homolog **5** (*Fig. 6*, ● *vs.* ○). Original fluorescence kinetics for ANTS/DPX efflux through pore **6** are shown in *Fig. 7* to demonstrate that changes in activity with

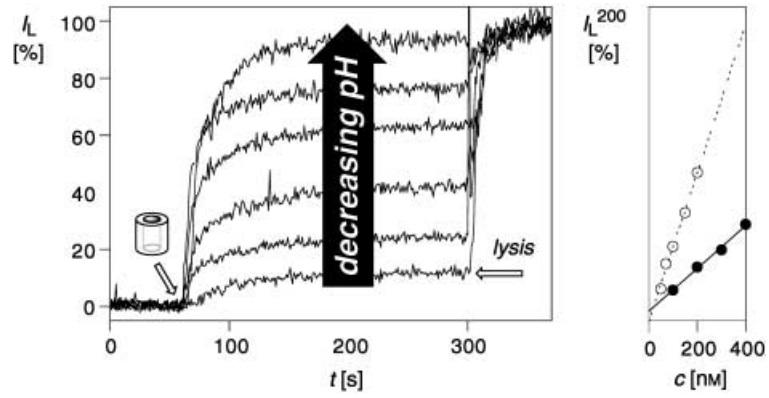

Fig. 7. *ANTS/DPX Efflux from EYPC SUVs through* p-*octiphenyl β-barrel* **6** *at* c = *50 n*M (*c* = 200 nM for monomer **6**^{m}) *at pH 4.5 – 7.0* (*cf. Fig. 6*) *and with increasing monomer concentration* (○) *compared to homolog* **5** (●, pH 5.5). I_L according to *Eqn. 4* (*Exper. Part*).

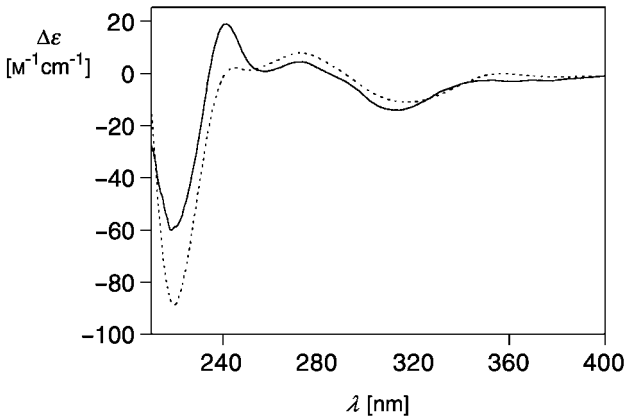

Fig. 8. *Circular dichroism spectra of homologous* p-*octiphenyl β-barrels* **6** (---), [15]) *and* **5** (—) *in* H_2O *at pH 5.5.*

pH were, as for all described barrels, substantial, clean, and complete. The characteristic shape of flux traces is representative for an 'all-or-none' mechanism [8][10][12][20][21][3], and the linear concentration dependence of ANTS/DPX efflux [8][10][12][20][21][3] provided valuable corroborative evidence for the existence of β-barrel **6** in both bilayer membranes as well as in H_2O [14–16]. Similar CD spectra for β-barrels **5** and **6** in buffer (*Fig. 8*) and linear concentration dependence of ANTS/DPX efflux (*Fig. 7*, ●) indicated that the same accounts for contracted homolog **5**. The 3.0-times increased activity in the ANTS/DPX assay of *labile* barrel **6** compared to *stable* barrel **5** originated presumably from less hindered dye efflux across the larger pores (*Fig. 7*, ● *vs.* ○).

The pH dependence of rigid-rod β-barrel **6** observed in the ANTS/DPX assay was corroborated and refined by exploiting its esterolytic activity [14]. Rigid-rod β-barrel **6** catalyzes the hydrolysis of CB-Ac [27][28] at pH 5.5 with a proficiency of $9.6 \cdot 10^5$ compared to 4(5)-methyl-1*H*-imidazole in H_2O [14][29]. In the presence of EYPC bilayers, intact esterolytic activity was observed under conditions where ion channels were active as well. Esterolytic activity of functional ion channels was further supported by evidence for CB binding to ion channels **6** in single-channel and multichannel experiments [14]. To obtain pH profiles for esterase **6** in EYPC bilayers, catalyst **6** was added to EYPC SUVs loaded with substrate CB-Ac. Because catalyst and substrate approach the bilayer from opposite sides, this experimental configuration was dubbed '*trans*' catalysis (*Fig. 9*, left). It contrasts to '*cis*' catalysis, where catalyst and substrate were added to a suspension of 'empty' EYPC SUVs (*Fig. 9*, right).

Esterolytic activity was quantified at different pH by determining the initial velocity of product formation from the increase in HPTS (= 8-hydroxypyrene-1,3,6-trisulfonic acid trisodium salt) emission with time [14][28]. The pH profile for '*trans*' esterolysis (●) was consistent with the pH profile for pore formation obtained from the ANTS/DPX assay (○, *Fig. 9*). The decrease in esterase activity at pH < 5 reflected, with all likelihood, the reduced availability of the catalytic nucleophiles/bases within barrel **6** rather than barrel 'explosion'. The bell-shaped pH profile for '*cis*' catalysis was nearly identical with the previously reported pH profile in H_2O at higher substrate

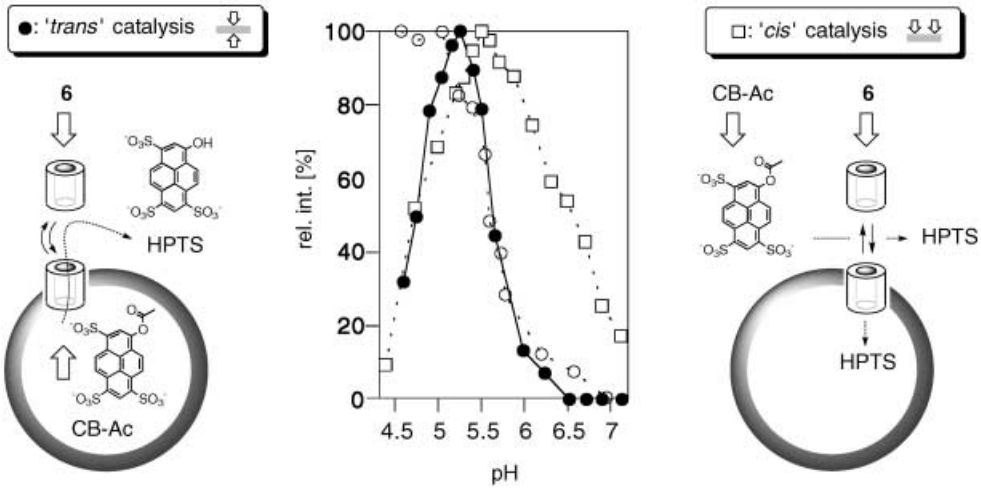

Fig. 9. *pH Profiles for* 'trans' (●) *and* 'cis' (□) *esterolysis of CB-Ac* (240 nM) *by* p-*octiphenyl* β*-barrel* **6** (135 nM, rel. int. = v_0/v_0(max); v_0(max) = 35 ± 17 pM/s (●) and 19 ± 2 pM/s (□)) *compared to ANTS/DPX efflux* (○) *with EYPC SUVs* (0.5 mM)

concentration (□, *Fig. 9*). The clearly higher relative but also absolute activity for '*cis*' compared to '*trans*' catalysis at pH > 5.4 may support previous observations in circular dichroism studies with aspartate-rich barrel **4** [12] that the *ICR* required to prevent barrel 'implosion' is smaller in H_2O than in membranes. However, comprehensive comparison of the pH profiles for '*cis*' and '*trans*' catalysis is non-trivial and beyond the scope of this report[3]).

As for aspartate-rich barrels **4**, pH profiles of histidine-rich barrels **5** and **6** implied that intermediate $7 < ICR < 12$ is required for activity and that poor $ICE < 7$ causes barrel implosion[4]). Nearly superimposable pH profiles of histidine-rich barrels **5** and **6**

---

[3]) In brief, the slightly higher activity for '*trans*' catalysis at pH < 5.4 adds, although poorly reproducible, strength to the hypothesis [15] that transmembrane (TM) substrate gradients may enhance the activity of ion-channel catalysts. Clearly higher activity for '*cis*' esterolysis at pH > 5.4 suggests the following: *1*) Pore **6** is not released to the intravesicular media within the timescale of esterolysis. This excludes toroidal pore formation from reversible interfacial binding and agrees with TM barrel-stave pores as expected from previous results [8–17]. *2*) Catalytic activity of barrel **6** may occur in the extravesicular media at 5.4 < pH < 7. This would suggest that less *ICR* is required in H_2O than in membranes to prevent barrel 'implosion' as noted previously with aspartate-rich barrel **4** [12]. Alternatively (or in addition), this may suggest that 'imploded' aqueous (AQ) barrels can be 'opened' by CB-Ac templates. *3*) Alternative (or in addition) to *2*), catalytic activity of barrel **6** at 5.4 < pH < 7 may occur within TM pores **6**. This may suggest that '*cis*' but not '*trans*' CB-Ac templates assist in the formation of open TM pores **6** at 5.4 < pH < 7. Indications for CB-template-assisted formation of ion channels **6** have been observed in planar EYPC bilayers by single-channel conductance experiments (unpublished); indications for template effects in *p*-octiphenyl β-barrel structure have been noted previously for carotenoids [9], RNA, and Zn^{2+} [15]. Overall, '*cis*' but not '*trans*' esterolysis at pH > 5.4 can be explained with either 'implosion' of TM (but not AQ) barrels **6** caused by external bilayer templates or 'opening' of TM and/or AQ barrels caused by internal CB templates. Further studies are needed to clarify these issues.

[4]) Indications for complete identity of the two systems, that is 'explosion' of β-barrel **6** with excessive $ICR_{3.5} > 12$, were noted previously by circular-dichroism spectroscopy [15].

suggested that barrel formation at intermediate $ICR_{5.0}$ is governed by proximity effects at *p*-octiphenyl turns (*a* and *b* in *Fig. 2*). *Locally* reduced G_r by *ca.* 7 Å β-sheet spacers (*d* in *Fig. 2*) may, however, contribute to the poor stability of tetramer **6** [14–16] compared to ion channels **1**–**3** and **5**.

Counterion Effects. Among neglected parameters in the *ICR* model (*Fig. 1*) are pore-specific counterion effects. Experimental support for eventual relevance of counterion effects was obtained by Q-TOF-nano-electrospray ionization mass spectrometry (Q-TOF-nano-ESI-MS) with barrels **6**. In contrast to earlier direct observations of dimeric minibarrels by ESI-MS [17], the unusually labile barrels **6** [14–16] were denaturated under all employed conditions and detected as monomeric $1^3,2^3,3^2,4^3,5^2,6^3,7^2,8^3$-octakis(Gla-Leu-His-Leu-His-Leu-NH_2)-*p*-octiphenyl $\mathbf{6}^m$ (*Fig. 10*) [30]. Extensive adduct formation produced a base peak at *m*/*z* 6291 that was inconsistent with *m*/*z* 6105 expected for monomer $\mathbf{6}^m$. The same counterions were also observed in presence of 0.1 equiv. of pyrene-1,3,6,8-tetrasulfonate (PTS), a competitive inhibitor of β-barrel esterase **6** [14] (*Fig. 10,a*). However, the presence of 1.0 and 10.0 equiv. of PTS caused nearly complete disappearance of all adducts (*Fig. 10,b*). Counterion removal by PTS occurred without compensating appearance of peaks for PTS·$\mathbf{6}^m$ or PTS·**6** complexes (*Fig. 10,c*). This suggested that PTS binds *stronger* than the other counterions to intact barrels **6** in solution ($K_i = 0.5$ μM [14]), whereas PTS binding to monomers formed during denaturating electrospray ionization is *weaker than nonspecific counterion binding*. PTS Binding to barrel **6** and adduct formation with monomers $\mathbf{6}^m$ confirmed that counterion effects influence the characteristics of pores with internal charges. Preliminary results in our laboratory and comparison with pertinent amphiphilic α-helix bundles [21] suggest that counterion effects within synthetic pores may be most pronounced with internal arginine residues.

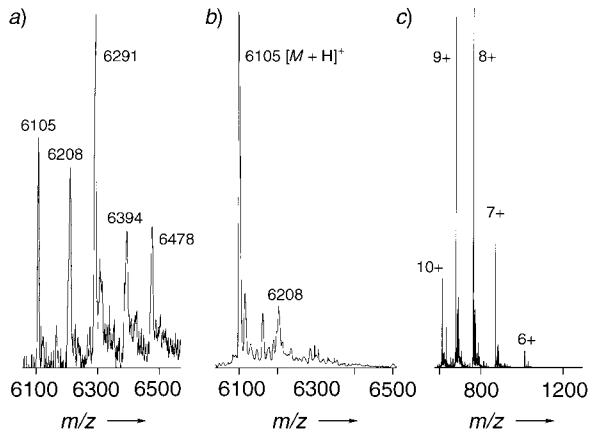

Fig. 10. *Q-TOF-Nano-electrospray ionization mass spectra of* $\mathbf{6}^m$*, calculated from the distribution of multiply-charged ions at* m/z = *700–1100, in the presence of* a) *0.1 and* b) *10 equiv. of pyrene-1,3,6,8-tetrasulfonate* (PTS); c) *original spectrum for* b)

Comparison with De Novo *α-Helix Bundles and Natural Ion Channels.* Pore formation of *p*-octiphenyl β-barrels can not be compared to *de novo* β-barrels due to

the unresolved synthesis of the latter from first principles [19]. Pore formation by synthetic, lysine-rich β-sheet peptides has, however, been reported [31]. Early studies with poly(VK) indicated, unlike LKL barrel **1**, slow and nearly pH-independent β-sheet formation at intermediate ionic strength in H_2O [32] (V = valine, K = lysine, L = leucine).

Pore formation by self-assembly of *de novo* designed amphiphilic α-helical peptides into expanded bundles or 'α-barrels' with a hydrophobic exterior and internal charges has been studied for decades. The overall characteristics of *de novo* 'α-barrels' and *p*-octiphenyl β-barrels of comparable design are surprisingly different. Unlike lysine-rich barrels **1**, *e.g.*, a weak decrease from 100 to 70% activity around pH 7.0 for lysine-rich amphiphilic α-helices (named KALA) in PC vesicles does not continue to 0% activity at low pH [22]. Unlike histidine-rich barrels **5** and **6**, pores formed by histidine-rich *de novo* α-helices (named LAH_4) exhibit poor pH dependence in PC vesicles [23]. Unlike aspartate-rich β-barrel **4**, pores formed by glutamate-rich *de novo* α-helices (named GALA) have a sigmoidal pH profile similar to histidine-rich β-barrels **5** and **6** with high activity at low rather than intermediate *ICR* [20].

Surprisingly, some characteristics of *p*-octiphenyl β-barrel pores were similar to natural ion channels rather than *de novo* 'α-barrels'. The colicin E1 channel, *e.g.*, remains a rare example where intermediate electrostatic interactions and activity have been correlated previously [33]. Variability of internal charges without global structural change has been demonstrated with, *e.g.*, alamethicin 'α-barrels' [24] and porin β-barrels [34]. Apparent increase in activity of the cystic fibrosis transmembrane conductance regulator (CFTR) with decreasing pH has been observed with histidine and glutamate in place of an internal arginine [35]. The M2 channel from influenza-A virus, a four-helix bundle with internal histidine residues [36–38], and histidine-rich barrels **5** and **6** rather than histidine-rich α-helices LAH_4 [23] share pH profiles and the ability of internal molecular recognition (antiviral adamantan-1-amine for M2). The structural model proposed for pH gating by internal histidine residues in M2 could (including [36] or excluding [38] additional cation-π interactions) contribute to the activation of histidine-rich barrels **5** and **6** at pH $\leq$ 5.5 as well.

Cooperatively gated activity of multifunctional *p*-octiphenyl β-barrel pores with internal lysine, aspartate, and histidine residues at intermediate *ICR*, dependent on β-sheet height and length as well as the surrounding media, is thus overall unlike *de novo* 'α-barrels' but similar to aspects of biological channels. This result supports original expectations from rigid-rod molecules in bioorganic chemistry, *i.e.*, that minimized axial molar entropy will maximize the preorganization of more complex, multifunctional supramolecular nanoarchitecture [39].

We thank *A. Pinto*, *J.-P. Saulnier*, the group of Prof. *F. Gülaçar*, and Dr. *H. Eder* for NMR, MS, and elemental analyses, respectively, and the *Swiss National Science Foundation* (21-57059.99, 2000-064818.01, and National Research Program 'Supramolecular Functional Materials' 4047-057496) for financial support.

Experimental Part

General. See [40]. CD Spectra: *Jasco 710* spectropolarimeter; $\Delta\varepsilon$ values refer to monomeric *p*-oligophenyls. Data analyses and pK_a simulations were made with KaleidaGraph 3.5. Compounds, abbreviations, and sources: ANTS, 8-aminonaphthalene-1,3,6-trisulfonic acid disodium salt (*Molecular Probes*); CB-Ac, cascade blue acetate = 8-acetoxypyrene-1,3,6-trisulfonic acid trisodium salt (*Fluka*); DPX, *p*-xylenebis[pyridinium] bromide

(*Molecular Probes*); EYPC, egg-yolk phosphatidylcholine (*Avanti*); *G*, $-OCH_2CO-$; H–*G*–OH, glycolic acid; H, L-histidine = His; HPTS, 8-hydroxypyrene-1,3,6-trisulfonic acid trisodium salt (*Fluka*); *ICE*, internal charge excess; *ICR*, internal charge repulsion; K, L-lysine = Lys; L, L-Leucine = Leu; MES, 2-morpholinoethanesulfonic acid monohydrate (*Fluka*); PTS, 1,3,6,8-pyrenetetrasulfonic acid tetrasodium salt (*Fluka*); SUVs, small unilamellar vesicles; TES, *N*-[tris(hydroxymethyl)methyl]-2-aminoethanesulfonic acid (*Fluka*) = 2-{[2-hydroxy-1,1-bis(hydroxymethyl)ethyl]amino}ethanesulfonic acid; TM, transmembrane; Tr, Trityl.

Syntheses. The monomers **1**^{m}–**6**^{m} for self-assembly of barrels **1**–**6** were prepared as described previously. Synthesis of $1^3,2^3,3^2,4^3,5^2,6^3,7^2,8^3$-octakis(*G*-Leu-His-Leu-His-Leu-NH_2)-*p*-octiphenyl **6**^{m} was as in [14] (supporting information), synthesis of $1^3,2^3,3^2,4^3,5^2,6^3,7^2,8^3$-octakis(*G*-Leu-Asp-Leu-Asp-Leu-NH_2)-*p*-octiphenyl **4**^{m} as in [12] (supporting information), synthesis of 1^4-methoxy-8^4-(methylsulfonyl)-$2^2,3^3,4^2,5^3,6^2,7^3$-hexakis(*G*-Leu-Lys-Leu-NH_2)-*p*-octiphenyl **3**^{m} and $1^4,8^4$-dimethoxy-$2^2,3^3,4^2,5^3,6^2,7^3$-hexakis(*G*-Leu-Lys-Leu-NH_2)-*p*-octiphenyl **2**^{m} as in [8] (supporting information), and synthesis of $1^3,2^3,3^2,4^3,5^2,6^3,7^2,8^3$-octakis(*G*-Leu-Lys-Leu-NH_2)-*p*-octiphenyl **1**^{m} as in [10][1]. Along the same route, **5**^{m} was prepared (see below).

*$1^3,2^3,3^2,4^3,5^2,6^3,7^2,8^3$-Octakis(*G*-Leu-His(Tr)-Leu-NH_2)*-p-*octiphenyl (= 1,1′,1″,1‴,1⁗,1⁗′,1⁗″,1⁗‴-[[1,1′:4′,1″:4″,1‴:4,1⁗:4⁗,1⁗′:4⁗′,1⁗″:4⁗″,1⁗‴:4⁗‴-octiphenyl]-2″,2‴,2⁗′,3,3′,3‴3⁗′,3⁗″-octayloctakis[oxy-(1-oxoethane-2,1-diyl)]}octakis[*L*-leucyl-N^{1}-(triphenylmethyl)-*L*-hystidyl-*L*-leucinamide]*). The $1^3,2^3,3^2,4^3,5^2,6^3,7^2,8^3$-Octa(*G*-OH)-*p*-octiphenyl [14] (2.9 mg, 2.4 μmol), *O*-benzotriazolyl-*N,N,N′,N′*-tetramethyluronium hexafluorophosphate (HBTU; 11 mg, 29 μmol), and Et_3N (62 μmol, 5 μl) were added to a soln. of H-Leu-His(Tr)-Leu-NH_2 [14] (23.3 mg, 37 μmol) in DMF (3 ml). After stirring for 2.5 h in the dark at r.t., the mixture was evaporated and washed with H_2O. Purification by CC (CH_2Cl_2/MeOH 8:1, R_f 0.5), solid/liquid extraction with CH_2Cl_2/MeOH 20:1, and prep. TLC (toluene/MeOH 3:1, R_f 0.2) yielded pure title compound (5 mg, 35%). Colorless solid. HPLC (*YMC-Pack SIL*, 50 × 4 mm, CH_2Cl_2/MeOH 94:6, 2 ml/min): t_R 12.5 min. ^{1}H-NMR (400 MHz, $CDCl_3/CD_3OD$ 1:1): 7.27–7.19 (*m*, 104 H); 7.01–6.96 (*m*, 48 H); 6.85–6.70 (*m*, 2 H); 6.64–6.40 (*m*, 8 H); 4.52–4.26 (several *m*, 40 H); 2.98–2.80 (*m*, 16 H); 1.58–1.21 (*m*, 48 H); 0.86–0.60 (*m*, 96 H). ESI-MS (2% AcOH/MeOH): 2014.2 (100, $[M+3\,H]^{3+}$).

*$1^3,2^3,3^2,4^3,5^2,6^3,7^2,8^3$-Octakis(*G*-Leu-His-Leu-NH_2)*-p-*octiphenyl (= 1,1′,1″,1‴,1⁗,1⁗′,1⁗″,1⁗‴-{[1,1′:4′,1″:4″,1‴:4⁗,1⁗′:4⁗′,1⁗″:4⁗″,1⁗‴:4⁗‴-octiphenyl]-2″,2⁗′,2⁗″′,3,3′,3‴3⁗′,3⁗″-octayloctakis[oxy(1-oxoethane-2,1-diyl)]}octakis[*L*-leucyl-*L*-hystidyl-*L*-leucinamide]; **5**^{m})*. The $1^3,2^3,3^2,4^3,5^2,6^3,7^2,8^3$-Octakis(*G*-Leu-His(Tr)-Leu-NH_2)-*p*-octiphenyl (4 mg, 0.66 μmol) was stirred in CF_3COOH for 2 h at r.t. After evaporation, the crude product was purified by HPLC (*YMC-Pack ODS-A*, 50 × 4 mm, H_2O/MeOH(1% CF_3COOH) 1:4, 1 ml/min, t_R 8.11 min): pure **5**^{m} (2.7 mg, quant.). Colorless solid. ^{1}H-NMR (400 MHz, CD_3OD, 25°): 8.12–7.96 (*m*, 4 H); 7.78–7.69 (*m*, 4 H); 7.46–7.25 (*m*, 32 H); 6.85–6.70 (*m*, 2 H); 4.72–4.63 (*m*, 8 H); 4.33–4.18 (*m*, 32 H); 2.91–3.12 (*m*, 16 H); 1.61–1.42 (*m*, 48 H); 0.95–0.69 (*m*, 96 H). ESI-MS (2% AcOH/MeOH): 2052 (25, $[M+2\,H]^{2+}$), 1369 (100, $[M+3\,H]^{3+}$), 1027 (40, $[M+4\,H]^{4+}$).

ANTS/DPX Assay. EYPC SUVs (68 ± 4 nm) were prepared by the dialytic detergent-removal technique by means of a *Mini Lipoprep*®(*AmiKa Corp*) as described previously [8][10–13]. In brief, a soln. of EYPC (50 mg in 50 μl of EtOH) and sodium cholate (22.4 mg; *Sigma*) in 950 μl of buffer *A* was dialyzed against 50 ml of buffer *A* (> 6 h, 5 mM TES, 12.5 mM ANTS, 45.0 mM DPX, 20 mM KCl, pH 7.0) and 1000 ml of buffer *B* (> 12 h, 5 mM TES, 100 mM KCl, pH 7.0), purified by gel filtration (*Sephadex G-50*, buffer *B*), and diluted to 6 ml. ANTS/DPX Efflux was recorded as a function of time by measuring changes in emission intensity I_t (λ_{em} 510 nm, λ_{ex} 353 nm [12][20][22], *FluoroMax-2*; *Jobin Yvon-Spex*) during the addition of the above EYPC-SUV suspension (10 mM EYPC, 50 μl) to stirred, thermostated buffer *C* (1.95 ml, 10 mM MES, 100 mM KCl, pH 4.5–7.0) to give emission intensity I_0, concentrated stock solns. of barrels **1**, **5**, and **6** (in 20–40 μl of MeOH, final monomer concentrations 0 nM–10 μM), and 10% aq. *Triton X-100* soln. (50 μl) to give emission intensity I_∞. Multichannel controls (λ_{em} 510 nm, $\lambda_{ex}(1)$ 360 nm, $\lambda_{ex}(2)$ 380 nm, $\lambda_{ex}(3)$ 400 nm) were run during each experiment to eliminate (not observed) unrelated contributions. Flux curves were normalized to percent leakage I_L^t by *Eqn. 4*, with I_t, I_0, and I_∞ as defined above. Dependence on pH, concentration, and external blockers was determined by plotting the leakage I_L^t [%] after a meaningful period of time (usually 200–250 s, *cf. Fig. 7*), *i.e.*, $I_L^2 00$ [%], as a function of the parameter of interest.

$$I_L = (I_t - I_0) / (I_\infty - I_0) \times 100\% \quad (4)$$

Esterolysis. For *cis*-catalysis, EYPC SUVs were prepared as above with buffer *C* (10 mM MES, 100 mM KCl) at pH 7.0 exclusively. Esterolysis was recorded (λ_{em} 510 nm; λ_{ex} 415.5 nm (pH controls: λ_{ex} 404 nm, 455 nm [14][28])) during addition of SUVs (50 μl), **6** (in 20–40 μl MeOH), and CB-Ac (in 20 μl buffer *C*) to buffer *C* (1.95–2.00 ml, pH 4.5–7.0). Absolute changes in product concentration with time were quantified from changes

in HPTS emission intensity by comparison with calibration curves. For *trans*-catalysis, EYPC SUVs were prepared as above with buffer *D* (10 mM MES, 100 mM KCl, 1 mM CB-Ac, pH 5.5, instead of *A*) and buffer *C* (instead of *B*). Intravesicular substrate concentrations in the final SUV suspensions were determined from the rate of hydrolysis by 4(5)-methyl-1*H*-imidazole ($k = 0.0032\ M^{-1}s^{-1}$) after lysis (10% aq. *Triton X-100* soln., 50 µl). Influence of mixed *Triton X-100*/EYPC micelles was negligible. *trans*-Esterolysis was recorded and analyzed as described for *cis*-esterolysis (without external addition of CB-Ac).

Q-TOF-nano-ESI-MS. A soln. of **6** (2.5 nM; 10 nM **6**^{m}) in MeOH/H_2O 6.5 : 3.5 with 0.1% formic acid and 0.1 nM (*Fig. 10*, *a*), 10 nM, and 100 nM PTS (*Fig. 10*, *b* and *c*) was measured with a Q-TOF mass spectrometer (*Micromass*, Manchester, UK), equipped with a nano-electrospray ion source.

REFERENCES

[1] B. Baumeister, Thèse No. 3302, Université de Genève, 2001.

[2] Reviews: G. W. Gokel, A. Mukhopadhyay, *Chem. Soc. Rev.* **2001**, *30*, 274; G. J. Kirkovits, C. D. Hall, *Adv. Supramol. Chem.* **2000**, *7*, 1; S. Matile, *Chem. Soc. Rev.* **2001**, *30*, 158; G. W. Gokel, *Chem.–Eur. J.* **2001**, *7*, 33; N. Sakai, S. Matile, *Chem.–Eur. J.* **2000**, *6*, 1731; G. W. Gokel, *Chem. Commun.* **2000**, 1; D. Seebach, M. G. Fritz, *Int. J. Biol. Macromol.* **1999**, *25*, 217; R. N. Reusch, *Biochemistry (Moscow)* **2000**, *65*, 335; Y. Kobuke, *Adv. Supramol. Chem.* **1997**, *4*, 163; G. W. Gokel, O. Murillo, *Acc. Chem. Res.* **1996**, *29*, 425; T. M. Fyles, W. F. van Straaten-Nijenhuis, in 'Comprehensive Supramolecular Chemistry', Ed. N. D. Reinhouldt, Elsevier, Oxford, 1996, Vol. 10 f., 53; N. Voyer, *Top. Curr. Chem.* **1996**, *184*, 1; J. D. Hartgerink, T. D. Clark, M. R. Ghadiri, *Chem. Eur. J.* **1998**, *4*, 1367; D. T. Bong, T. D. Clark, J. R. Granja, M. R. Ghadiri, *Angew. Chem., Int. Ed.* **2001**, *40*, 988; U. Koert, *Chem. Unserer Zeit* **1997**, *31*, 20; J.-H. Fuhrhop, J. Köning, 'Membranes and Molecular Assemblies: The Cytokinetic Approach', The Royal Society of Chemistry, Cambridge, UK, 1994; R. J. M. Nolte, *Chem. Soc. Rev.* **1994**, 11; K. S. Åckerfeldt, J. D. Lear, Z. R. Wasserman, L. A. Chung, W. F. DeGrado, *Acc. Chem. Res.* **1993**, *26*, 191.

[3] Recent publications: V. Janout, I. V. Staina, P. Bandyopadhyay, S. L. Regen, *J. Am. Chem. Soc.* **2001**, *123*, 9926; P. Bandyopadhyay, V. Janout, L.-H. Zhang, S. L. Regen, *J. Am. Chem. Soc.* **2001**, *123*, 7691; P. H. Schlesinger, R. Ferdani, J. Liu, J. Pajewska, R. Pajewski, M. Saito, H. Shabany, G. W. Gokel, *J. Am. Chem. Soc.* **2002**, *124*, 1848; L. M. Cameron, T. M. Fyles, C. Hu, *J. Org. Chem.* **2002**, *67*, 1548; T. M. Fyles, R. Knoy, K. Müllen, M. Sieffert, *Langmuir* **2001**, *17*, 6669; T. M. Fyles, C. Hu, R. Knoy, *Org. Lett.* **2001**, *3*, 1335; V. Sidorov, F. W. Kotch, G. Abdrakhmanova, R. Mizani, J. C. Fettinger, J. T. Davis, *J. Am. Chem. Soc.* **2002**, *124*, 2267; A. J. Wright, S. E. Matthews, W. B. Fischer, P. D. Beer, *Chem.–Eur. J.* **2001**, *7*, 3474; C. Goto, M. Yamamura, A. Satake, Y. Kobuke, *J. Am. Chem. Soc.* **2001**, *123*, 12152; N. Yoshino, A. Satake, Y. Kobuke, *Angew. Chem., Int. Ed.* **2001**, *40*, 457; H.-D. Arndt, A. Knoll, U. Koert, *ChemBioChem* **2001**, *2*, 221; H.-D. Arndt, A. Knoll, U. Koert, *Angew. Chem., Int. Ed.* **2001**, *40*, 2076; J. Sanchez-Quesada, H. S. Kim, M. R. Ghadiri, *Angew. Chem., Int. Ed.* **2001**, *40*, 2503; E. Biron, N. Voyer, J. C. Meillon, M.-E. Cormier, M. Auger, *Biopolymers* **2001**, *55*, 364; N. Sakai, D. Gerard, S. Matile, *J. Am. Chem. Soc.* **2001**, *123*, 2517; C. Pérez, C. G. Espínola, C. Foces-Foces, P. Núñez-Coello, H. Carrasco, J. D. Martín, *Org. Lett.* **2000**, *2*, 1185.

[4] I. Tabushi, Y. Kuroda, K. Yokota, *Tetrahedron Lett.* **1982**, *23*, 4601; S. J. Kennedy, R. W. Roeske, A. R. Freeman, A. M. Watanabe, H. R. Besch Jr, *Science (Washington, D.C.)* **1977**, *196*, 1341.

[5] D. Wang, L. Guo, J. Zhang, L. R. Jones, Z. Chen, C. Pritchard, R. W. Roeske, *J. Peptide Res.* **2001**, *57*, 301.

[6] J. A. Mindell, H. Zhan, P. D. Huynh, R. C. Collier, A. Finkelstein, *Proc. Natl. Acad. Sci. U.S.A.* **1994**, *91*, 5272; H. Bayley, C. R. Martin, *Chem. Rev.* **2000**, *100*, 2575.

[7] X. S. Xie, H. P. Lu, *J. Biol. Chem.* **1999**, *274*, 15967.

[8] N. Sakai, S. Matile, *J. Am. Chem. Soc.* **2002**, *124*, 1184; N. Sakai, D. Houdebert, S. Matile, *Chem.–Eur. J.*, submitted.

[9] B. Baumeister, S. Matile, *Chem.–Eur. J.* **2000**, *6*, 1739.

[10] B. Baumeister, N. Sakai, S. Matile, *Angew. Chem., Int. Ed.* **2000**, *39*, 1955.

[11] N. Sakai, B. Baumeister, S. Matile, *ChemBioChem* **2000**, *1*, 123.

[12] G. Das, S. Matile, *Proc. Natl. Acad. Sci. U.S.A.* **2002**, *99*, 5183.

[13] A. Som, N. Sakai, S. Matile, *Bioorg. Med. Chem.*, submitted.

[14] B. Baumeister, N. Sakai, S. Matile, *Org. Lett.* **2001**, *3*, 4229.

[15] B. Baumeister, S. Matile, *Macromolecules* **2002**, *35*, 1549.

[16] G. Das, L. Ouali, M. Adrian, B. Baumeister, K. J. Wilkinson, S. Matile, *Angew. Chem., Int. Ed.* **2001**, *40*, 4657.

[17] N. Sakai, N. Majumdar, S. Matile, *J. Am. Chem. Soc.* **1999**, *121*, 4294.

[18] M. D. Levin, P. Kaszynski, J. Michl, *Chem. Rev.* **2000**, *100*, 169; P. F. H. Schwab, M. D. Levin, J. Michl, *Chem. Rev.* **1999**, *99*, 1863; A. J. Berresheim, M. Müller, K. Müllen, *Chem. Rev.* **1999**, *99*, 1747; R. E. Martin, F. Diederich, *Angew. Chem., Int. Ed.* **1999**, *38*, 1351; J. M. Tour, *Chem. Rev.* **1996**, 96, 537.
[19] J. D. Stevenson, S. Lutz, S. J. Benkovic, *Angew. Chem., Int. Ed.* **2001**, *40*, 1854; J. A. Gerlt, *Nat. Struct. Biol.* **2000**, ***7***, 171; N. Nagano, E. G. Hutchinson, J. M. Thornton, *Protein Sci.* **1999**, *8*, 2072; D. R. Flower, *Biochem. J.* **1996**, *318*, 1; J. S. Richardson, *Nature (London)* **1977**, *268*, 495; S. K. Buchanan, *Curr. Opin. Struct. Biol.* **1999**, *9*, 445; G. Pujadas, J. Palau, *Biologia (Bratislava)* **1999**, *54*, 231; M. H. Hecht, *Proc. Natl. Acad. Sci. U.S.A.* **1994**, *91*, 8729.
[20] N. K. Subbarao, R. A. Parente, F. C. Szoka Jr., L. Nadasdi, K. Pongracz, *Biochemistry* **1987**, *26*, 2964; R. A. Parente, S. Nir, F. C. Szoka Jr., *Biochemistry* **1990**, *29*, 8720; F. Nicol, S. Nir, F. C. Szoka Jr., *Biophys. J.* **2000**, *78*, 818.
[21] S. Lee, T. Tanaka, K. Anzai, Y. Kirino, H. Aoyagi, G. Sugihara, *Biochim. Biophys. Acta* **1994**, *1191*, 181; T. Iwata, S. Lee, O. Oishi, H. Aoyagi, M. Ohno, K. Anzai, Y. Kirino, G. Sugihara, *J. Biol. Chem.* **1994**, *269*, 4928; S. Stankowski, M. Pawlak, E. Kaisheva, C. H. Robert, G. Schwarz, *Biochim. Biophys. Acta* **1994**, *1191*, 77; U. Silphaduang, E. J. Noga, *Nature (London)* **2001**, *414*, 268.
[22] T. B. Wyman, F. Nicol, O. Zelphati, P. V. Scaria, C. Planck, F. C. Szoka Jr., *Biochemistry* **1997**, *36*, 3008; M. Dathe, T. Wieprecht, H. Nikolenko, L. Handel, W. L. Maloy, D. L. MacDonald, M. Beyermann, M. Bienert, *FEBS Lett.* **1997**, *403*, 208; M. Dathe, M. Schürmann, T. Wieprecht, A, Winkler, M. Beyermann, E. Krause, K. Matsuzaki, O. Murase, M. Bienert, *Biochemistry* **1996**, *35*, 12612.
[23] T. C. B. Vogt, B. Bechinger, *J. Biol. Chem.* **1999**, *274*, 29115.
[24] V. Borisenko, M. S. P. Sansom, G. A. Woolley, *Biophys. J.* **2000**, *78*, 1335; D. P. Tieleman, J. Breed, H. J. C. Berendsen, M. S. P. Sansom, *Faraday Discuss.* **1998**, *111*, 209.
[25] B. Dietrich, M. W. Hosseini, J.-M. Lehn, R. B. Sessions, *J. Am. Chem. Soc.* **1981**, *103*, 1282.
[26] C. C. Cruickshank, R. F. Minchin, A. C. Le Dain, B. Martinac, *Biophys. J.* **1997**, *73*, 1925.
[27] J. E. Whitaker, R. P. Haugland, P. L. Moore, P. C. Hewitt, M. Reese, R. P. Haugland, *Anal. Biochem.* **1991**, *198*, 119.
[28] O. S. Wolfbeis, E. Koller, *Anal. Biochem.* **1983**, *129*, 365.
[29] T. Sazaki, M. Lieberman, 'Protein Mimetics', in 'Comprehensive Supramolecular Chemistry', Vol. 4, Ed. Y. Murakami, Elsevier, Oxford, 1996, p. 193; H. Dugas, 'Bioorganic Chemistry', Springer, New York, 1996; A. Tramontano, K. D. Janda, R. A. Lerner, *Science (Washington, D.C.)* **1986**, *234*, 1566; S. J. Pollack, P. G. Schultz, *J. Am. Chem. Soc.* **1989**, *111*, 1929; K. S. Broo, H. Nilson, J. Nilson, L. Balzer, *J. Am. Chem. Soc.* **1998**, *120*, 10287; J. P. Guthrie, J. Cossar, B. A. Dawson, *Can. J. Chem.* **1986**, *64*, 2456; J. M. K. Sanders, *Chem.–Eur. J.* **1998**, *4*, 1378.
[30] B. S. Kinnear, M. R. Hartings, M. F. Jarrold, *J. Am. Chem. Soc.* **2001**, *123*, 5660.
[31] J. Blazyk, R. Wiegland, J. Klein, J. Hammer, R. M. Epand, R. F. Epand, W. L. Maloy, U. P. Kari, *J. Biol. Chem.* **2001**, *276*, 27899; S. Castano, B. Desbat, J. Dufourcq, *Biochim. Biophys. Acta* **2000**, *1463*, 65; S. Ono, S. Lee, H. Mihara, H. Aoyagi, T. Kato, N. Yamasaki, *Biochim. Biophys. Acta* **1990**, *1022*, 237.
[32] A. Brack, L. E. Orgel, *Nature (London)* **1975**, *256*, 383.
[33] S. D. Zakharov, J. B. Heymann, Y.-L. Zhang, W. A. Cramer, *Biophys. J.* **1996**, *70*, 2774.
[34] P. S. Phale, A. Philippsen, C. Widmer, V. P. Phale, J. P. Rosenbusch, T. Schirmer, *Biochemistry* **2001**, *40*, 6319.
[35] J. F. Cotton, M. J. Welsh, *J. Biol. Chem.* **1999**, *274*, 5429.
[36] A. Okada, T. Miura, H. Takeuchi, *Biochemistry* **2001**, *40*, 6053.
[37] L. H. Pinto, G. R. Dieckmann, C. S. Gandhi, C. G. Papworth, J. Braman, M. A. Shaughnessy, J. D. Lear, R. A. Lamb, W. F. DeGrado, *Proc. Natl. Acad. Sci. U.S.A.* **1997**, *94*, 11301.
[38] K. J. Schweighofer, A. Pohorille, *Biophys. J.* **2000**, *78*, 150.
[39] S. Matile, *Chem. Rec.* **2001**, *1*, 162.
[40] N. Sakai, D. Gerard, S. Matile, *J. Am. Chem. Soc.* **2001**, *123*, 2517 (supporting information at http://pubs.acs.org).

Received March 19, 2002